

Article

Mechanical Performance of Mortars with Partial Replacement of Cement by Aluminum Dross: Inactivation and Particle Size

Daniel Parra-Molina ¹, Manuel Alejandro Rojas-Manzano ¹, Adriana Gómez-Gómez ¹,
Mario Fernando Muñoz-Vélez ¹ and Aníbal Maury-Ramírez ^{1,2,*}

¹ Department of Civil and Industrial Engineering, Faculty of Engineering and Sciences, Pontificia Universidad Javeriana Cali, Calle 18# 118–250, Santiago de Cali 760031, Colombia; danielparra17@javerianacali.edu.co (D.P.-M.); alejandro.rojas@javerianacali.edu.co (M.A.R.-M.); adrianagomez@javerianacali.edu.co (A.G.-G.); mario.munoz@javerianacali.edu.co (M.F.M.-V.)

² Architecture Department, Faculty of Design Sciences, University of Antwerp, Mutsaardstraat 29, 2000 Antwerp, Belgium

* Correspondence: anibal.maury-ramirez@uantwerpen.be

Abstract: Although the use of primary aluminum dross as cement replacement has shown promising results in mortars and concretes, there is a knowledge gap between the effect of the secondary dross inactivation process and particle sizes on the mechanical properties and consistency. So, by using X-ray diffraction, laser granulometry, and scanning electron microscopy, this article describes first the inactivation process applied to a secondary aluminum dross. Second, this manuscript presents the fresh and hardened properties of mortar mixes containing 5, 10, and 20% inactivated secondary aluminum dross with three different particle sizes (i.e., fine, intermediate, and coarse). Mortar flow test results indicate that compressive and flexural strengths of mixes containing up to 20% fine and intermediate aluminum dross as cement replacement were satisfactory, respectively. These results have the potential to reduce the environmental and health impacts caused by cement production and secondary aluminum dross disposal, respectively. Moreover, the durability aspects of the mortar mixes, as well as the effectivity of the investigated inactivation process, are identified as future research topics.

Keywords: aluminum dross; eco-mortar; dross inactivation; dross particle size; mechanical properties; industrial symbiosis; circular economy; sustainable building materials; sustainable construction



Citation: Parra-Molina, D.; Rojas-Manzano, M.A.; Gómez-Gómez, A.; Muñoz-Vélez, M.F.; Maury-Ramírez, A. Mechanical Performance of Mortars with Partial Replacement of Cement by Aluminum Dross: Inactivation and Particle Size. *Sustainability* **2023**, *15*, 14224. <https://doi.org/10.3390/su151914224>

Academic Editor: Estefanía Cuenca Asensio

Received: 4 September 2023

Revised: 17 September 2023

Accepted: 21 September 2023

Published: 26 September 2023



Copyright: © 2023 by the authors. Licensee MDPI, Basel, Switzerland. This article is an open access article distributed under the terms and conditions of the Creative Commons Attribution (CC BY) license (<https://creativecommons.org/licenses/by/4.0/>).

1. Introduction

Although there are significant environmental impacts at local and global scales, the construction sector is strongly connected to economic growth and social development by promoting a large number of jobs (direct and indirect) and energizing other subsectors of the economy [1]. The last is particularly important in developing countries such as Colombia, which was ranked third (13 Mt), after Brazil (56.6 Mt) and Mexico (40.0 Mt), based on cement production in Latin America and the Caribbean [2]. So, in order to minimize the environmental impacts while increasing social development and economic growth, the City Hall of Santiago de Cali is evaluating the implementation of a circular economy model for the construction sector, which understands circular economy (CE) as a production and consumption system that promotes efficiency in the use of materials, water, and energy, taking into account the resilience of ecosystems and the circular use of material flows through the implementation of technological innovations, alliances, and collaborations between stakeholders (e.g., raw material producers, building companies, users, and final disposal actors) and the promotion of business models that respond to the fundamentals of sustainable development [3]. Among other strategies, the CE model stimulates the use of eco-concretes and eco-mortars that replace cement with by-products from local industries [4].

Aluminum dross is a by-product of aluminum production that can be classified based on the aluminum content in white (15 to 70% Al), black (12 to 18% Al), and salt cake (3 to 5% Al). Most frequently, white aluminum dross is reprocessed due to its high quality. On the other hand, black dross and aluminum salt cake, which are normally landfilled, have been investigated in building materials as additive, calcium aluminate cement, cement, and fine aggregate replacements [5] (Figure 1).

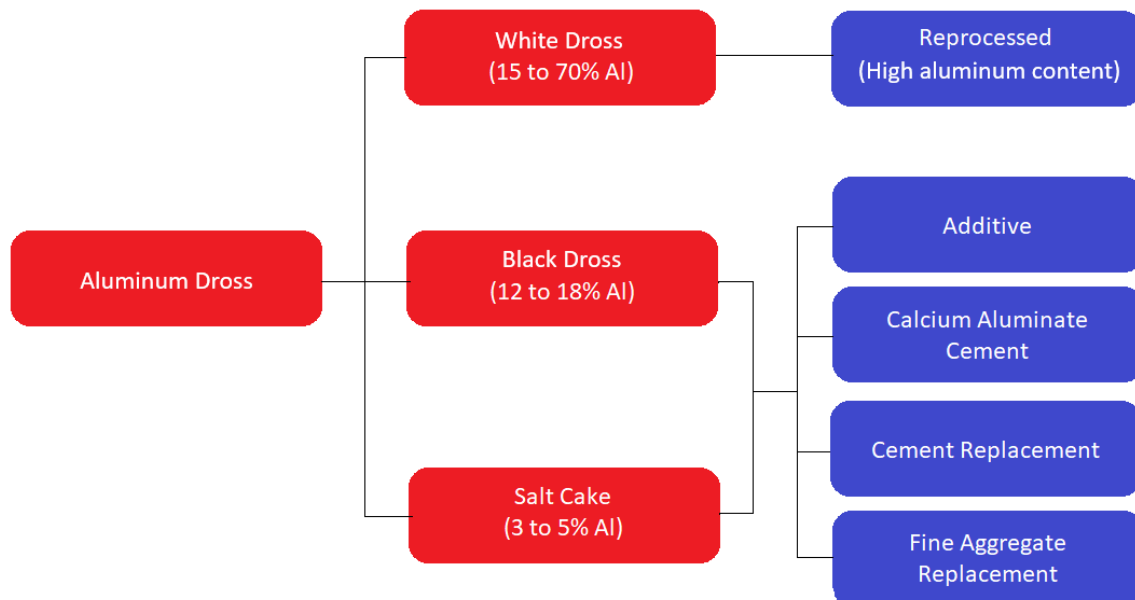


Figure 1. Some aluminum dross uses in building materials [5].

Pereira et al. (2000) investigated the use of salt cake, containing oxides of aluminum, as a replacement for cement and sand in mortars. They reported satisfactory cement replacement around 10% and sand replacement from 30% to 50% [6]. As supplementary cementitious materials, Elinwa and Mbadike (2011) produced concrete by replacing various percentages of cement with aluminum waste. From their results, it was found that the compressive and flexural strengths of concrete with replacement levels of 10 to 15% are comparable to those of control concrete. Another result was that concrete-containing aluminum waste retards the concrete setting times, which is desirable for hot-weather concreting [7]. Similarly, Reddy & Neeraja (2016) studied the use of aluminum dross as a cement replacement in concrete. They reported that for up to 15% replacement of cement by secondary aluminum dross, the performance is comparable with conventional concrete [8]. In the same way, Mailar et al. (2016) reported superior mechanical and durability properties with a concrete by replacing 20% of the cement with aluminum dross. They also noticed a delay in the setting process [9]. Additionally, Panditharadhya et al. (2018) investigated the partial replacement of Portland cement with aluminum dross (5%, 10%, 15%, and 20%) and its combined use with a pozzolan in concrete. They reported that by increasing the percentage of dross, the mixture required more water to keep a normal consistency. They also found that as the percentage of dross replacement increased, the initial setting time increased, but the final setting time decreased. Regarding the mechanical properties, they observed that as the percentage of cement substitution increased, the compressive, tensile, and flexural strengths decreased, an aspect that was associated with the increase of voids in the mixture by the addition of dross [10]. A detailed compilation of these results is presented in Table 1.

Table 1. Results from mortars and concretes using aluminum dross and salt cake as supplementary cementitious materials.

Reference	Material with Aluminum By-Products as Cement Phase	Compressive Strength	Flexural Strength	Consistency Indicated by the Setting Time
[6]	Mortar with 10% aluminum salt cake	↔	↔	N.A.
[7]	Concrete with 10 to 15% aluminum dross	↔	↔	↑
[8]	Concrete with 15% aluminum dross	↔	↔	N.A.
[9]	Concrete with 20% aluminum dross	↑	↑	↑
[10]	Concrete with 5%, 10%, 15% and 20% aluminum dross	↓	↓	↓

↑: Increase, ↓: Decrease, ↔: Not affected.

Although the above-mentioned aluminum dross and salt cake valorization experiences are significantly important for sustainable development, as they reduce Portland cement consumption and mitigate landfill-associated problems, the relationship between the dross characteristics and the mechanical performance of the investigated building materials is not completely clear. In this sense, it is quite important to understand the aluminum dross inactivation process, which will certainly impact the dross properties and, therefore, the mechanical performance of building materials using this by-product. For example, Dai and Apelian (2017) used primary (rich in aluminum and magnesium) and secondary (complex impurities mixture) aluminum dross in cement mortars and studied the effect of particle size, weight fraction, and dross origin on the mechanical properties of mortar specimens. Obtaining only promising results with the primary dross, they concluded that these factors have important effects on the uniformity of the microstructure of mortar specimens [11]. Therefore, this research aims to fill the knowledge gap in the relationship between secondary aluminum dross inactivation and particle size and the mechanical performance of mortars containing 5, 10, and 20% aluminum dross as cement replacement.

2. Materials and Methods

The proposed methodology for this study consisted of five phases, which are (1) Preliminaries, (2) By-product Characterization, (3) Mix Design, (4) Mortars and Properties, and (5) Results Analysis (Figure 2). It is noteworthy that the Colombian norms—NTC standards—are an adaptation of the American Society for Testing and Materials (ASTM) standards (Appendix A) and were used in this project. A brief description of each phase is presented as follows:

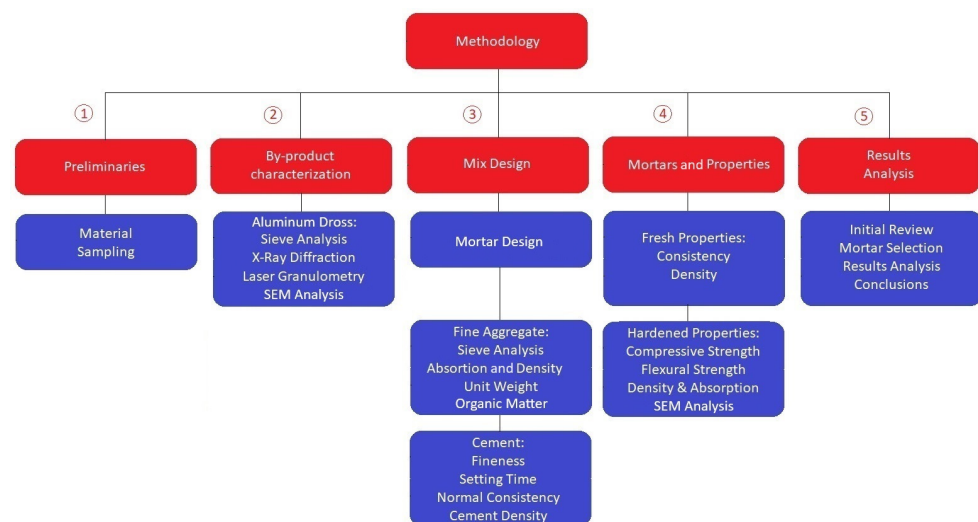


Figure 2. Methodology, which includes five phases: (1) Preliminaries, (2) By-product Characterization, (3) Mix Design, (4) Mortars and Properties, and (5) Results Analysis. Adapted from [12].

The first phase included all the preliminary activities to obtain the materials for mortar manufacturing. In this case, river sand from the Cauca River (fine aggregate), high early strength cement (Argos), and aluminum dross—a by-product obtained from a local aluminum industry—were selected. The chemical properties of the cement are presented in Appendix B, which is based on a quality control report done by the producer during the project.

The second phase aimed to exclusively characterize the aluminum dross by means of sieve analysis, X-ray diffraction (Rigaku Multiflex with Search/Match analysis), SEM—Scanning Electron Microscopy (Japanese Manufacturer of Scientific Instruments JEOL Model JSM-6490)—and laser granulometry (Malvern Instruments Model Mastersizer 2000). The X-ray diffraction measurements were obtained with Bragg-Brentano geometry and $\text{Cu K}\alpha$. The angular range was $2\theta = 6^\circ$ – 110° in steps of 0.02° , and the counting time was 8 s/step. SEM analysis at $100\times$, $1000\times$, and $5000\times$ on gold-coated samples was employed to examine the morphology. The particle-size measurements were conducted using the laser diffraction method with wet dispersion in water. The characterization of aluminum dross was done before and after inactivation and also after grinding to obtain the fine ($\leq 75 \mu\text{m}$), intermediate (75–150 μm), and coarse particle sizes (150–300 μm).

The aim of the third phase was the mortar mix design using characterization of the fine aggregate and cement. The mix design methodology was developed by Sánchez de Guzmán [13] and requires definition of a goal of compressive strength and consistency, which in this case were 28 MPa and plasticity over 110% in the mortar test flow. Additionally, this methodology requires the characterization of all components, which in this case was done through sieve analyses (NTC 77), absorption and density (NTC 237 and 176), unit weight (NTC 92), and organic matter (NTC 127) for the fine aggregate characterization. Similarly, fineness (NTC 33), setting time (NTC 118), normal consistency (NTC 110), and density (NTC 221) were used for the cement [14–21].

In the fourth phase, after the mix design was obtained for the reference mortar, mixes with cement replacements of 5, 10, and 20% (on a weight basis) using aluminum dross with different particle sizes (fine, intermediate, and coarse) were manufactured. Investigated mixes were then evaluated using three replicates regarding their fresh and hardened properties using the consistency (NTC 5784), density (NTC 1926), compressive and flexural strengths (NTC 220 and NTC 120), SEM analyses, and density and absorption tests [22–25]. Thus, mix designations, descriptions, and sample numbers are presented in Table 2.

Table 2. Mortar mix designation, aluminum dross content, and particle size.

Mix Designation	Aluminum Dross Content (%)	Aluminum Dross Particle Size (μm)
REF	0	0
5F	5	Fine ($\leq 75 \mu\text{m}$)
5I	5	Intermediate (75–150 μm)
5C	5	Coarse (150–300 μm)
10F	10	Fine ($\leq 75 \mu\text{m}$)
10I	10	Intermediate (75–150 μm)
10C	10	Coarse (150–300 μm)
20F	20	Fine ($\leq 75 \mu\text{m}$)
20I	20	Intermediate (75–150 μm)
20C	20	Coarse (150–300 μm)

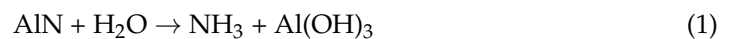
Lastly, the fifth phase consisted of analyzing the results for selecting the best-performance mortar mixtures in terms of the obtained mechanical properties and consistency. In this case, mix design and application criteria such as NTC–2017 were used to perform the analysis [26].

3. Results Analysis

3.1. Preliminary Activities

The aim of this phase was to obtain high-quality raw materials for the mortars, especially regarding the aluminum dross. Twenty-five kilograms of this by-product was obtained from a local industry that mainly produces aluminum profiles by primary and secondary processes that generate white dross, black dross, and salt cake. The dross used in this study is that which passes through a 2 mm sieve and is collected from different batches following the Orozco-Erao et al. (2022) procedure [27].

At the university laboratory, the aluminum dross inactivation was done by water immersion for 5 days, followed by drying in an oven at 115 to 120 °C for 24 h. In this process, which is represented by equation (1), water reacts with aluminum nitride (AlN) to form ammonia (NH₃) and aluminum oxide (Al₂O₃), as indicated by Shinzato & Hypolito (2005) [28]. Finally, the aluminum dross was exposed to air for 7 days. The whole process was also called dross washing due to the use of water as the main inactivator.



Afterwards, the dross was exposed to abrasion at the Los Angeles machine, which was operated at 1000 rpm with 12 iron balls for 30 min. Then, a separation process with sieves #50 (300 µm opening size), #100 (150 µm opening size), #200 (75 µm opening size), and a bottom sieve was performed to classify the different particle sizes required. More details from the aluminum dross collection and inactivation processes can be observed in Figure 3.



Figure 3. Aluminum dross collection and inactivation processes.

3.2. By-Product Characterization

3.2.1. Aluminum Dross Inactivation

The washing process or inactivation of the aluminum dross caused chemical and physical changes that were detected by XRD, SEM, and laser granulometry. First, there was a reduction in aluminum nitride (AlN) and formation of aluminum hydroxide (Al(OH)₃). This can be observed when comparing the XRD analyses after (a) and before (b) washing in Figure 4. There was a reduction in and appearance of peaks 2 and 6, respectively.

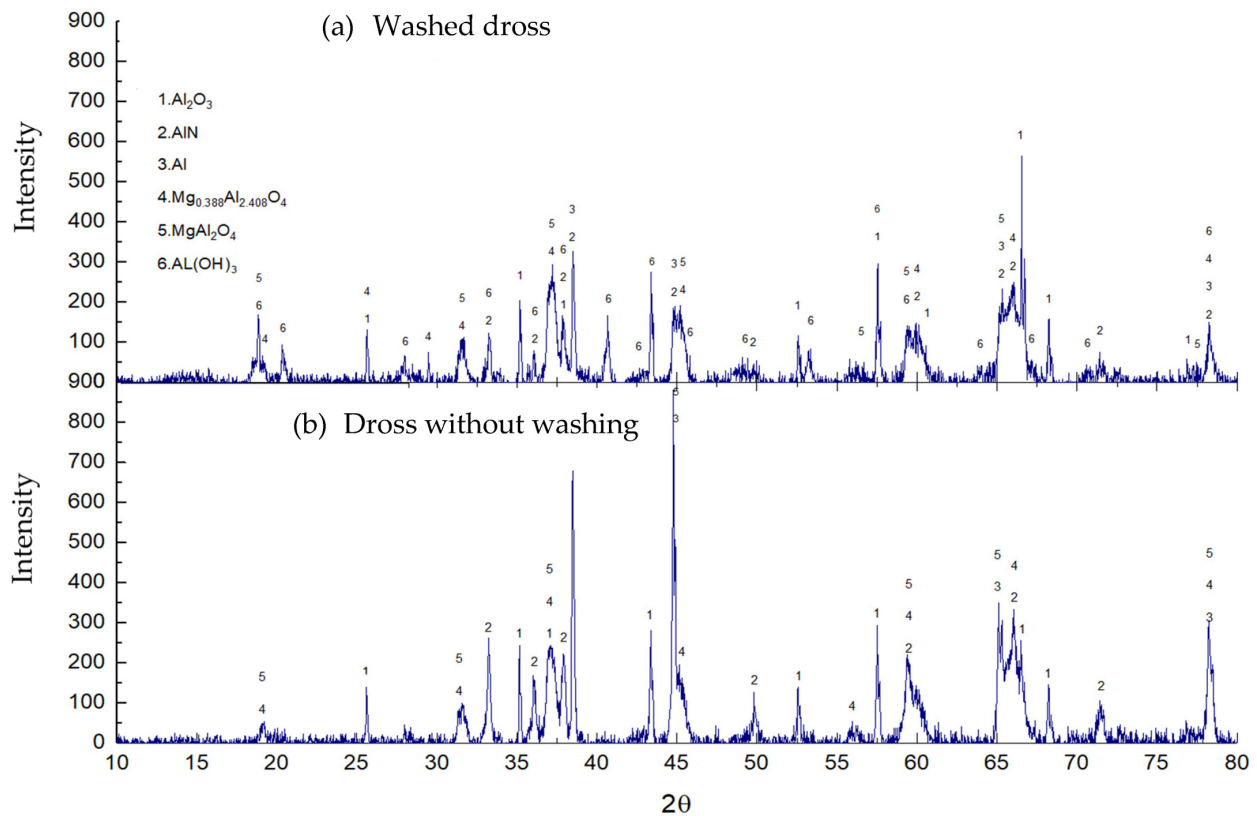


Figure 4. XRD analyses from aluminum dross washed (a) and without washing (b).

Second, there was agglomeration of the dross particles, which increased the particle size range from 20–800 μm to 100–1000 μm (Figure 5). Also, some morphological changes can be observed in Figure 6 with the SEM analyses at 100×, 1000×, and 5000× from aluminum dross washed (a) and without washing (b). The appearance of larger particles with softer surfaces (fiber type) after the aluminum dross inactivation is noticeable. Similarly, the increase in particle size due to dross inactivation can be observed in the higher specific surface area, uniformity coefficient, and average particle diameter that were calculated from the laser granulometry results and compiled in Table 3.

3.2.2. Aluminum Dross Grinding

Although the aluminum dross grinding did not cause chemical changes, there were significant ones in the physical properties, mainly particle size. Laser granulometry results indicate a particle size between 100 and 600 μm, with an average particle diameter of 234.9 μm for the coarse fraction of the aluminum dross. Similarly, a particle size between 30 and 300 μm, with an average particle diameter of 80.0 μm for the intermediate fraction. Also, a particle size between 1 and 100 μm, with an average particle diameter of 22.9 μm, was determined for the fine fraction (Figure 7).

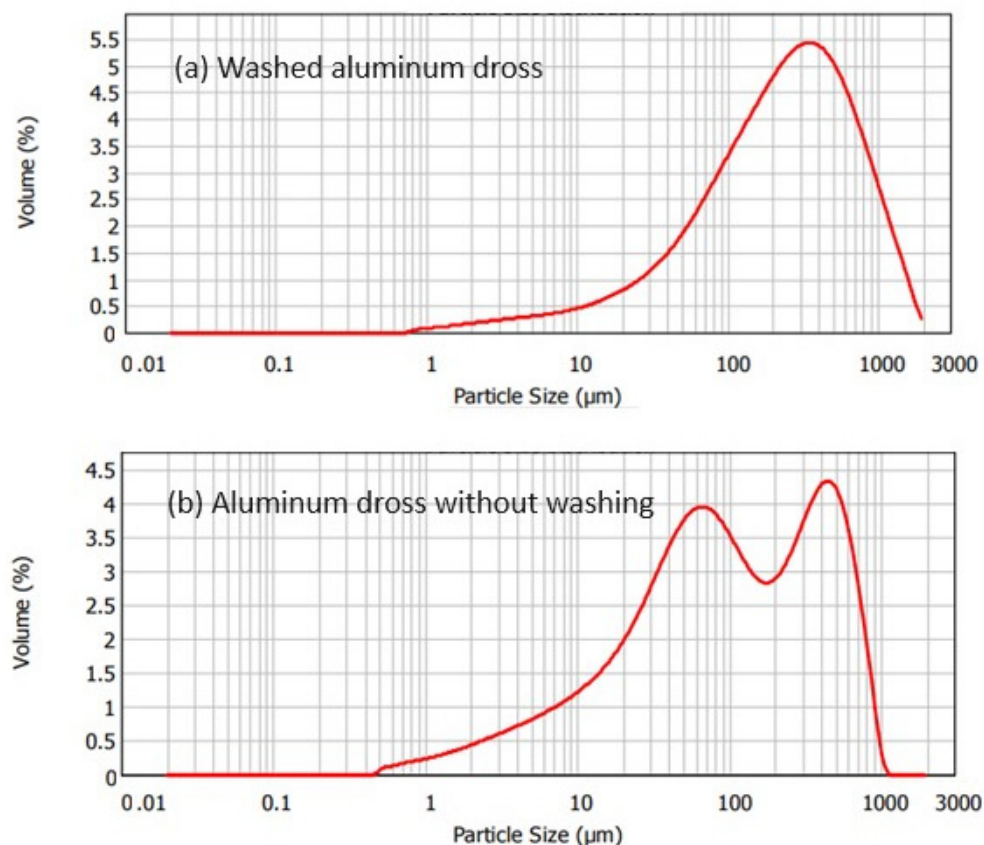


Figure 5. Particle-size distribution obtained by laser granulometry from aluminum dross washed (a) and without washing (b).

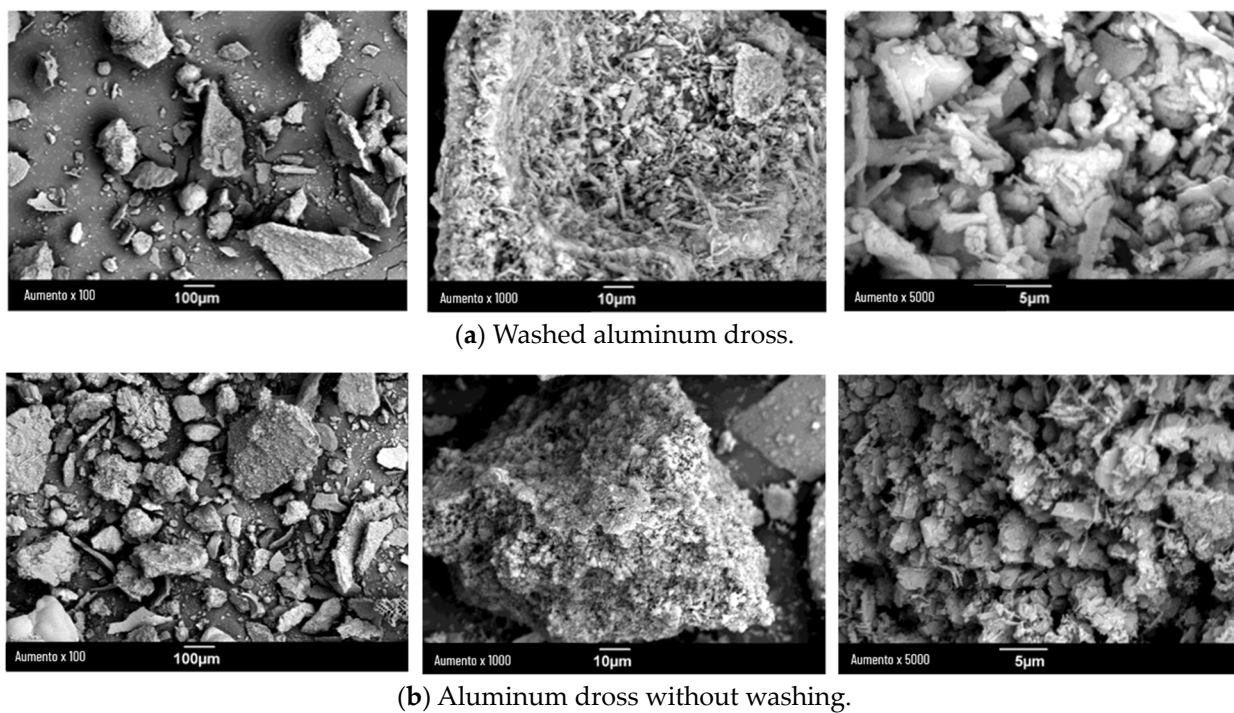
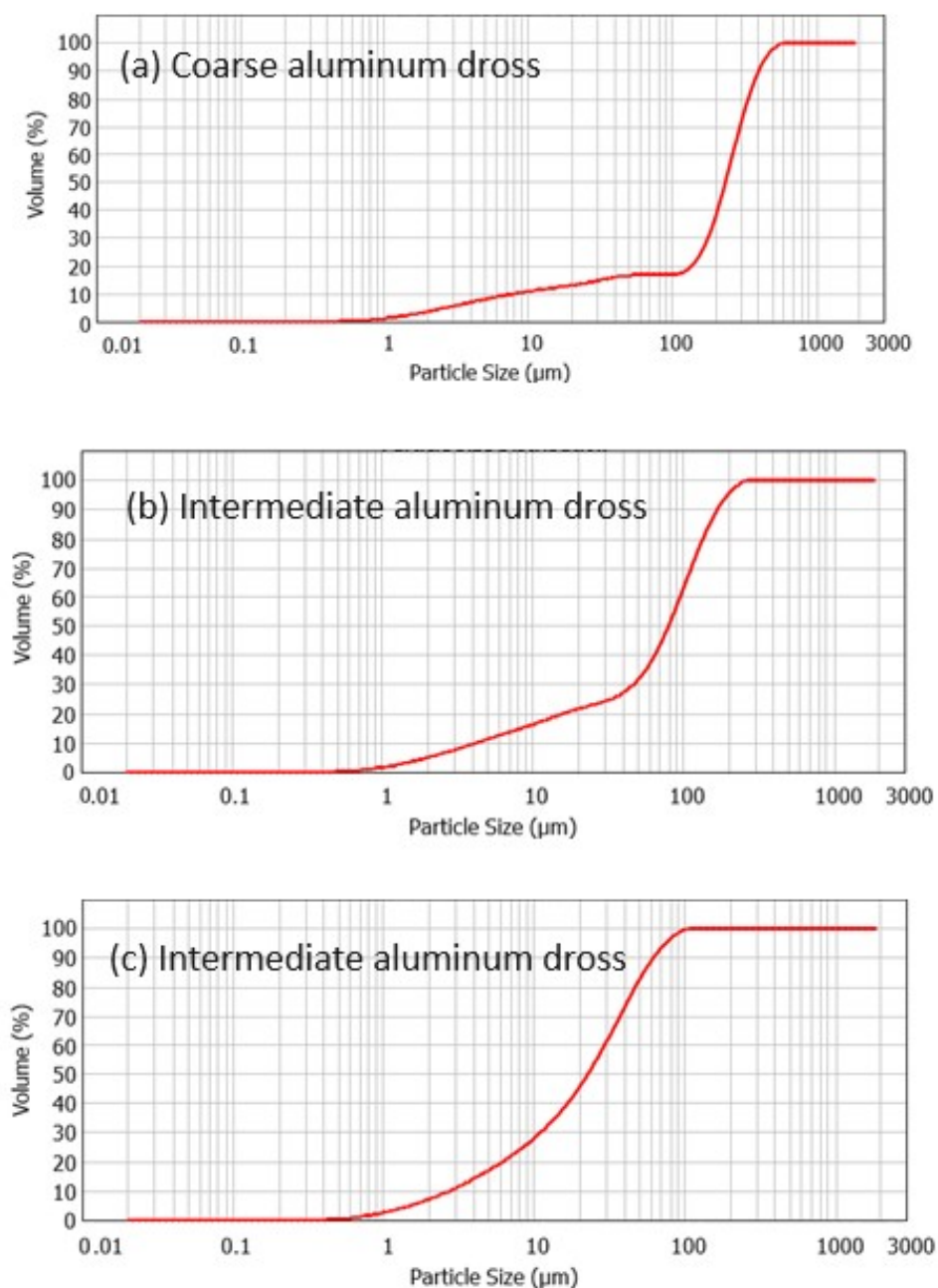


Figure 6. SEM analyses at 100 \times , 1000 \times , and 5000 \times from aluminum dross washed (a) and without washing (b).

Table 3. Specific surface, uniformity coefficient, and average particle diameter of aluminum dross at different conditions.

Dross Condition	Specific Surface (m ² /g)	Uniformity Coefficient	Average Particle Diameter (μm)
Washed dross	0.121	1.03	243.105
Dross without washing	0.316	1.71	92.432
Coarse dross (washed)	0.329	0.48	234.895
Intermediate dross (washed)	0.500	0.624	80.022
Fine dross (washed)	0.829	0.809	22.912

**Figure 7.** Particle-size distribution obtained by laser granulometry from coarse (a), intermediate (b), and fine (c) washed aluminum dross.

Additionally, a summary of the specific surface areas, uniformity coefficients, and average particle diameters of the three fractions is presented in Table 3. Considering that

the aluminum dross will be part of the cementitious phase in this research, it is important to compare these parameters with those obtained for the cement. In this context, with a specific surface of $0.342 \text{ m}^2/\text{g}$ ($3420 \text{ cm}^2/\text{g}$), cement is much more similar to coarse dross. Considering its uniform coefficient of 0.701, cement is much more similar to intermediate and fine dross. Also, in relation to its average particle diameter, fine dross almost doubles ($22.9 \mu\text{m}$) that of the used cement ($14.36 \mu\text{m}$).

3.3. Mix Design

Following the corresponding standards, first, the fine aggregate—which is river sand from the Cauca River (Colombia)—was physically characterized by calculating the sand density at saturated and surface-dried conditions, absorption, natural humidity, fineness modulus and nominal max. particle size. These two last parameters were calculated from the sieve analysis and granulometric curve presented in Figure 8. The parameters used in the reference mortar mix design are presented in Table 4.

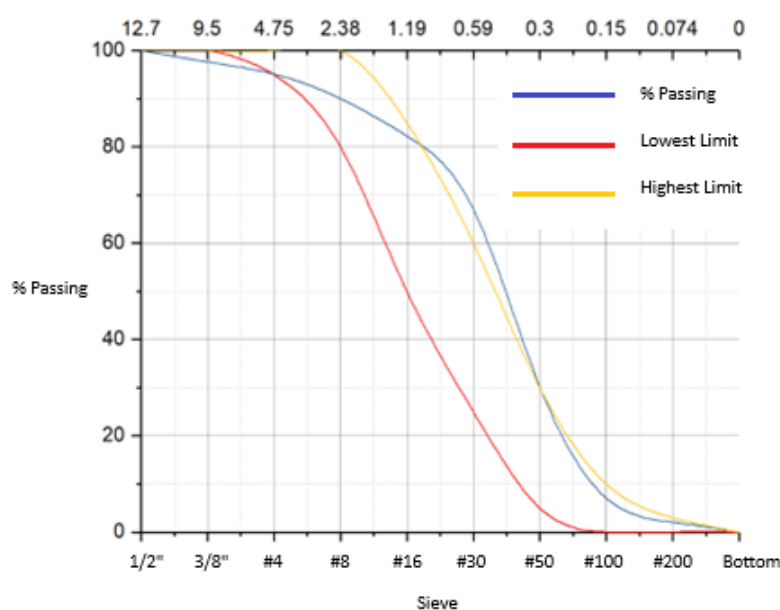


Figure 8. Granulometry analysis of fine aggregate.

Table 4. Physical parameters of the fine aggregate and cement used in the mortar mix design.

Parameter	Value
Sand density ^a	2.68 g/cm ³
Sand absorption	2.56%
Sand natural humidity	8.50%
Sand fineness modulus	2.31
Sand nominal max. particle size	4.75 mm (Sieve #4)
Initial setting time (cement)	53 min
Final setting time (cement)	195 min (3.25 h)
Cement density	2.88 g/cm ³

^a Fine aggregate at saturated and surface-dried conditions.

Second, the reference mortar composition was determined by the mix design method proposed by Sanchez Guzman (2011) [13], which requires defining the compressive strength (28 MPa) and consistency (plastic) of the mortar. So, using the physical characterization of the fine aggregate and cement, the following mix composition was defined for one cubic meter of reference mortar (Table 5). Then, mixes with cement replacements of 5, 10, and 20% aluminum dross (fine, intermediate, and coarse) were performed to this mix design.

Table 5. Components for one cubic meter of reference mortar with a compressive strength of 28 MPa and plastic consistency.

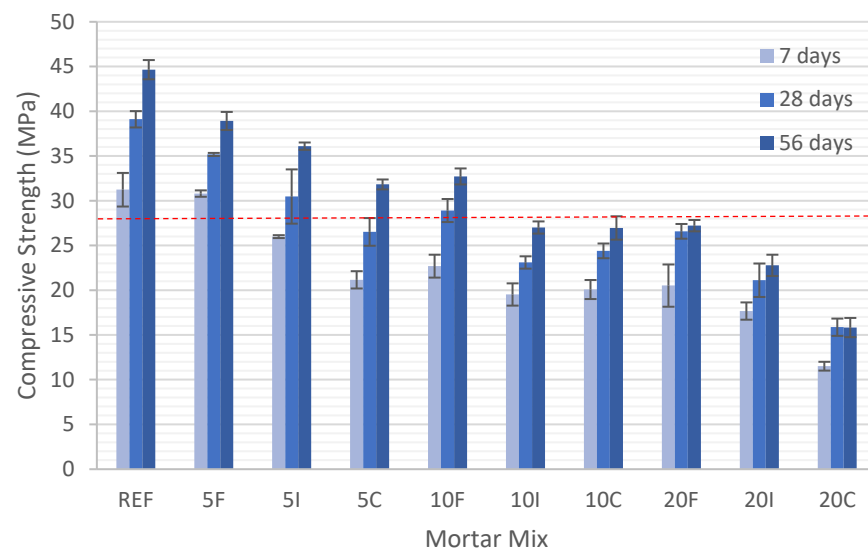
Component	Mass (kg)	Volume (L)
Fine aggregate	1255.0 ^a	467.94
Cement	550.0	190.97
Water	340.0	340.0

^a Fine aggregate at saturated and surface-dried conditions.

3.4. Fresh and Hardened Properties of Mortars

Mortar flow results show that mortar mixes with aluminum dross content up to 20% did not substantially affect their design consistencies, which were over 110% in all cases. However, there was a slight consistency decrease when increasing the aluminum dross content in the mortar mixes. These results are in agreement with those reported in [10], where there was a decrease in the consistency, indicated by a decrease in the final setting time.

On the other hand, the mechanical properties indicated by the compressive strength at 7, 28, and 56 days of the investigated mortar mixes are presented in Figure 9. Results show that mortar mixes containing up to 20% fine aluminum dross satisfy the required 28 MPa compressive strength after 28 and 56 days. On the contrary, samples using 20% aluminum dross with coarse and intermediate particle sizes did not satisfy the compressive strength required in the mix design. Although there was an increase in the mechanical performance after 7, 28, and 56 days of casting, this was not enough to achieve the required performance in these samples. This trend was also reported by Panditharadhya, Mulangi, and Shankar (2019), who studied concrete with 5%, 10%, 15%, and 20% aluminum dross [10].

**Figure 9.** Compressive strength at 7, 28, and 56 days from the different mortar mixes partially replacing cement (0, 5, 10, and 20%) with coarse (C), intermediate (I), and fine (F) aluminum dross.

Similar to the compressive strength, the flexural strength decreased with the aluminum dross content used in the mortar samples (Figure 10). In this case, mortar mixes containing up to 20% aluminum dross with fine and intermediate particle sizes have acceptable mechanical performances. For example, these satisfactorily comply with the minimum mechanical resistance required for paving stones (4.2 MPa according to the NTC 2017 standard). Similar flexural strengths were obtained recently by one of the authors using recycled aggregates obtained from old paving stones in Cauca (Colombia) [29].

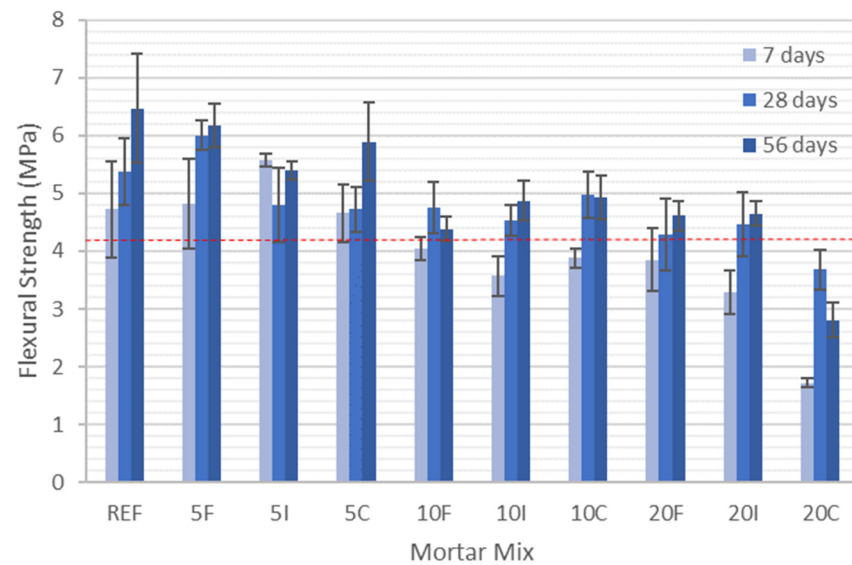


Figure 10. Flexural strength at 7, 28, and 56 days from the different mortar mixes partially replacing cement (0, 5, 10, and 20%) with coarse (C), intermediate (I), and fine (F) aluminum dross.

Moreover, when analyzing the correlation between the compressive and flexural strengths (Figure 11), it is observed that the compressive strength is between five and seven times the flexural strength, which is in agreement with other reported results. Similarly, the decreasing trend in the flexural and compressive strengths when increasing the amount of aluminum dross from 0% (REF) to 20% can be explained by the combined effect of the mortar porosity and dross particle sizes. Indeed, although not reflected in the density and absorption tests, there was a slight porosity increase observed in the SEM images at $100\times$, $2000\times$, and $5000\times$ of mortar samples (Figure 12). This porosity was produced by the residual gases (e.g., NH_3) released during the curing process by the aluminum dross. This can be confirmed through the XRD analyses (Figure 4), where there was a reduction in peaks 2 and 6, but still, there was not complete elimination of the aluminum nitride. However, compressive and flexural strengths reported here with the secondary aluminum dross are significantly higher than those reported by Dai and Apelian (2017) when evaluating mortars with 20% secondary dross. They reported a decrease in the mortar flexural strengths from 86 to 100% for fine and coarse particle sizes, respectively [11].

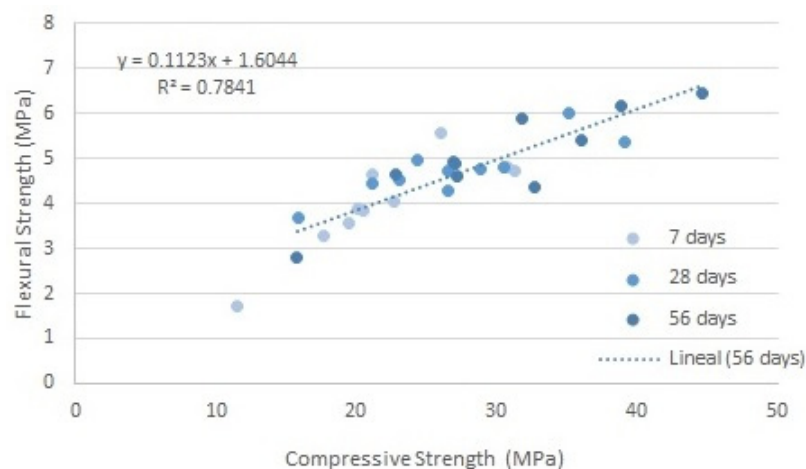


Figure 11. Relationship between the flexural and compressive strengths of mortar mixtures using aluminum dross as cement replacement (0, 5, 10, and 20%) with different particle sizes (F: Fine, I: Intermediate, C: Coarse).

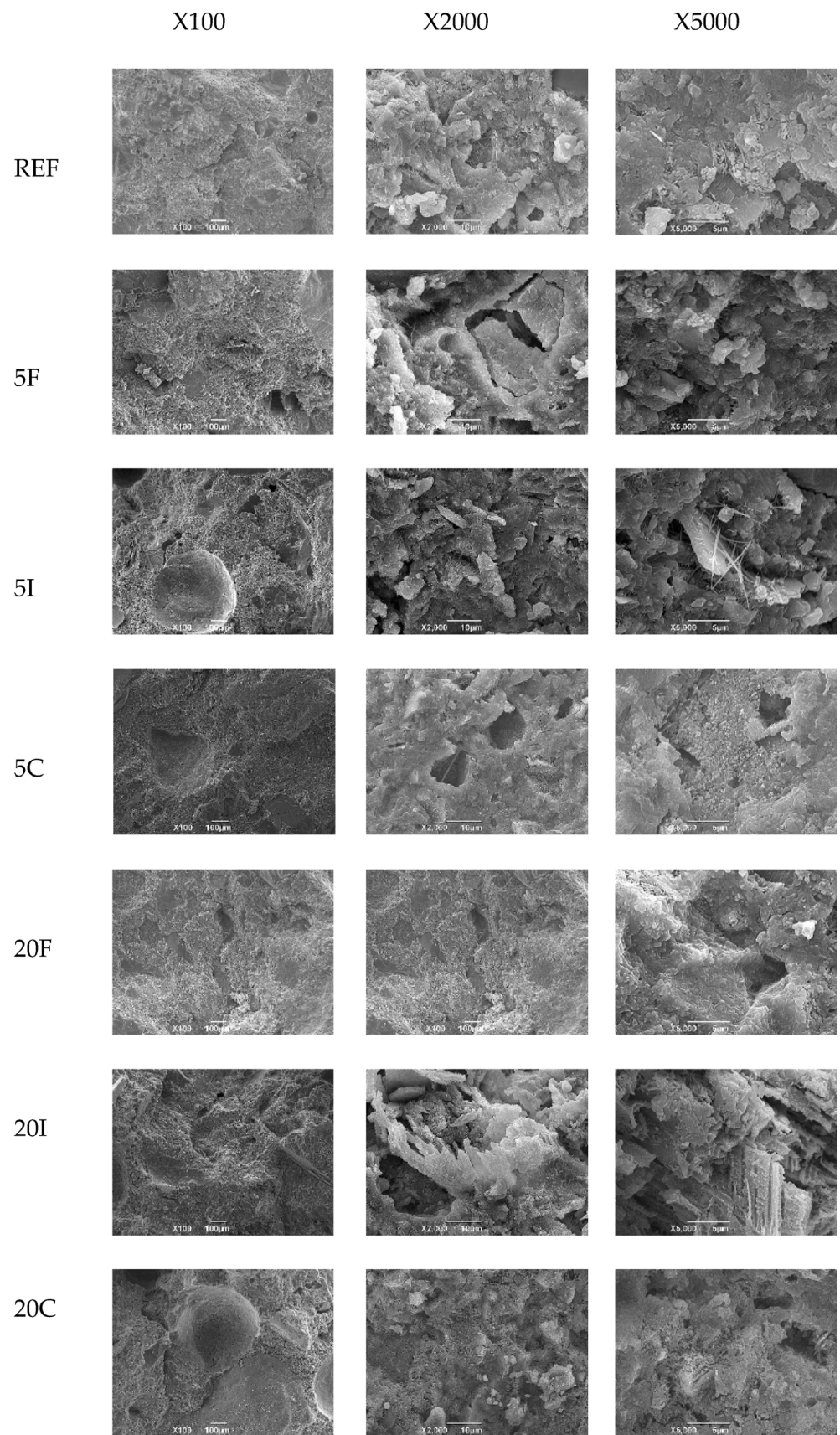


Figure 12. SEM images at 100 \times , 2000 \times , and 5000 \times of mortar mixes with partial replacement of cement with aluminum cross.

Finally, it must be pointed out that prior to real-scale application of the investigated mortars, their durability aspects and environmental impacts should be investigated to include a complete life-cycle approach to evaluation. Also, optimization of the dross inactivation process is identified as a key factor in significantly contributing to the net zero carbon program signed by Santiago de Cali, which is aimed at reducing the current and projected consumption of cement in Colombia, the third-largest CO₂ producer from cement in the Latin America region, after Brazil and Mexico (Figure 13) [30,31]. So, simultaneous research is currently being performed by the authors on the design of an industrial-scale production process and a financial feasibility analysis for a specific case study. The findings validated the potential of the proposed recovery process and provided insights into determining the market price for the resulting product [32].

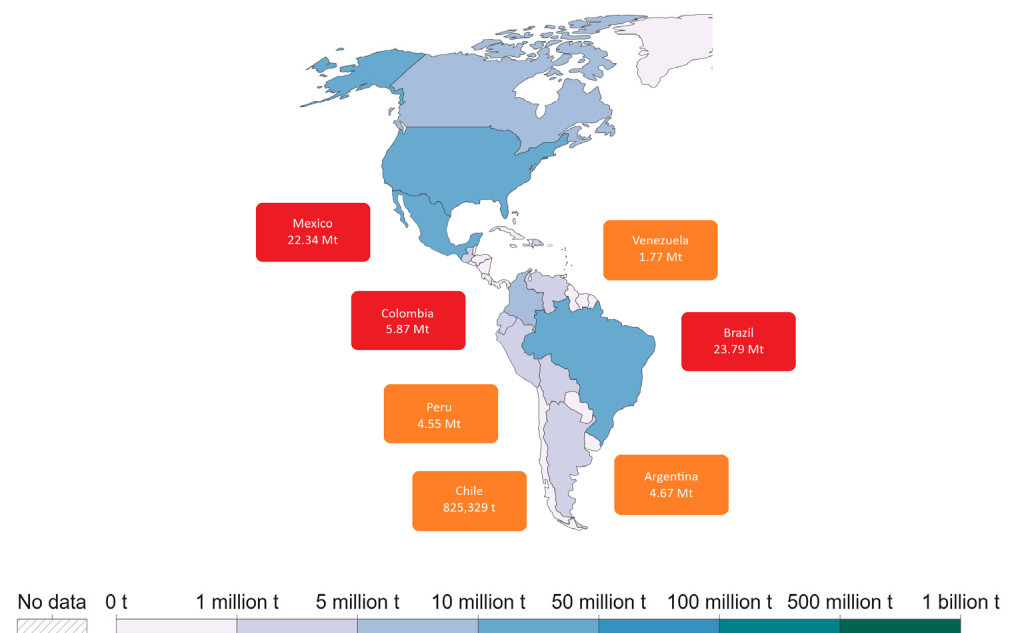


Figure 13. CO₂ emissions from cement in the Latin America region modified from Our World Data based on the Global Carbon Budget (2022) [30].

4. Conclusions

This article described first the inactivation of aluminum dross and second the evaluation of this aluminum dross with three different particle sizes as supplementary cementitious materials in mortar mixes designed for a compressive strength of 28 MPa and a plastic consistency of 110% in the mortar flow test. Mortar flow test results and compressive and flexural strengths of mortar mixes containing up to 20% fine and intermediate aluminum dross as cement replacement were satisfactory. However, mortar mixes containing 20% coarse aluminum dross did not satisfy the design applications. This might be attributed to the combined effect of a higher mortar porosity and large dross particle size. Mortar porosity was increased by the gases released by the aluminum dross during the curing process. Although aluminum nitride reacted with water to form ammonia and aluminum oxide during the aluminum dross inactivation process, there was still non-reacted AlN releasing gaseous NH₃ during the curing process of this mortar mix.

Although more research should be performed prior to the mortar's real-scale application, this article reports the importance of industrial symbiosis between the construction and aluminum industries from Santiago de Cali (Colombia) in reducing carbon dioxide emissions due to the lower consumption of cement. Also, this reports the use of aluminum dross as a supplementary cementitious material in mortars to reduce the potential impacts on the environment and public health caused by aluminum dross disposal.

Author Contributions: Conceptualization, M.A.R.-M., A.G.-G. and A.M.-R.; methodology, M.A.R.-M. and A.G.-G.; validation, D.P.-M., M.A.R.-M. and A.G.-G.; formal analysis, D.P.-M., M.A.R.-M. and A.G.-G.; investigation, D.P.-M., M.A.R.-M. and A.G.-G.; resources, M.F.M.-V.; data curation, A.M.-R.; writing—original draft preparation, A.M.-R.; writing—review and editing, A.M.-R.; visualization, D.P.-M. and A.M.-R.; supervision, M.F.M.-V.; project administration, M.F.M.-V.; funding acquisition, M.F.M.-V. All authors have read and agreed to the published version of the manuscript.

Funding: The authors would like to thank the financial support given by the internal call of Pontificia Universidad Javeriana Cali through the grant 2168-2021.

Institutional Review Board Statement: Not applicable.

Informed Consent Statement: Not applicable.

Data Availability Statement: Not applicable.

Acknowledgments: The authors would like to thank Alumina S.A. for providing the aluminum dross generated during the aluminum smelting processes. They also acknowledge the Servicio Geológico Colombiano sede Cali for allowing them to use their laboratories and equipment.

Conflicts of Interest: The authors declare no conflict of interest.

Appendix A

This section presents the equivalence between the NTC and ASTM Standards used in this research project (Table A1).

Table A1. Equivalence between NTC and ASTM standards.

NTC Standard	ASTM Standard
NTC-77 Método de ensayo para el análisis por tamizado de los agregados finos y gruesos	ASTM C136/C136M-19 Standard Test Method for Sieve Analysis of Fine and Coarse Aggregates
NTC-237 Método de ensayo para determinar la densidad relativa (gravedad específica) y la absorción del agregado fino	ASTM C128-22 Standard Test Method for Relative Density (Specific Gravity) and Absorption of Fine Aggregate
NTC-176 Método de ensayo para determinar la densidad relativa (gravedad específica) y la absorción del agregado grueso	ASTM C127-15 Standard Test Method for Relative Density (Specific Gravity) and Absorption of Coarse Aggregate
NTC-92 Método de ensayo para la determinación de la densidad volumétrica (masa unitaria) y vacíos en agregados	ASTM C29/C29M-17a Standard Test Method for Bulk Density (“Unit Weight”) and Voids in Aggregate
NTC-33 Método de ensayo para determinar la finura del cemento hidráulico por medio del aparato Blaine de permeabilidad al aire	ASTM C204-23 Standard Test Methods for Fineness of Hydraulic Cement by Air-Permeability Apparatus
NTC-118 Método de ensayo para determinar el tiempo de fraguado del cemento hidráulico mediante aguja de Vicat	ASTM C191-21 Standard Test Methods for Time of Setting of Hydraulic Cement by Vicat Needle
NTC-110 Cantidad de agua requerida para la consistencia normal de una pasta de cemento hidráulico	ASTM C187-23 Standard Test Method for Amount of Water Required for Normal Consistency of Hydraulic Cement Paste
NTC-221 Método de ensayo para determinar la densidad del cemento hidráulico	ASTM C188-17 Standard Test Method for Density of Hydraulic Cement
NTC-5784 Método de ensayo para determinar la fluidez de morteros de cemento hidráulico	ASTM C1437-20 Standard Test Method for Flow of Hydraulic Cement Mortar
NTC-1926 Método de ensayo para determinar la densidad (masa unitaria), el rendimiento y el contenido de aire por gravimetría del concreto	ASTM C138/C138M-23 Standard Test Method for Density (Unit Weight), Yield, and Air Content (Gravimetric) of Concrete
NTC-220 Determinación de la resistencia de morteros de cemento hidráulico a la compresión, usando cubos de 50 mm o 2 pulgadas de lado	ASTM C109/C109M-21 Standard Test Method for Compressive Strength of Hydraulic Cement Mortars (Using 2-in. or [50 mm] Cube Specimens)
NTC-120 Método de ensayo para determinar la resistencia a la flexión de morteros de cemento hidráulico	ASTM C348-21 Standard Test Method for Flexural Strength of Hydraulic-Cement Mortars
NTC-2017 Adoquines de concreto para pavimento	ASTM C1319-23 Standard Specification for Concrete Grid Paving Units

Appendix B

This section describes the chemical properties of the cement used in this project. This information comes from a quality control report performed by the cement producer from 1

to 30 September 2021 in the manufacturing plant located in Yumbo (Colombia). Table A2 presents the main cement phases and compounds statistically analyzed from thirty samples of cement. With 68%, C₃S (alite) and C₂S (belite) represent the major phases responsible for the mechanical performance. Similarly, the C₃A (aluminate) phase, which is lower than the maximum allowed (15%), is responsible for the early strength obtained. Finally, it is observed that the chemical compounds are among the limits established for cement durability. This is particularly important regarding MgO (periclase) and alkali compounds (K₂O and N₂O).

Table A2. Main cement phases and compounds of the cement used in this project.

Abbreviation	Average	SD	CV	Max	Min	Range
C ₃ S	53.91	1.07	1.98	56.65	52.25	4.40
C ₂ S	14.44	0.86	5.96	16.39	12.95	3.45
C ₄ AF	11.83	0.21	1.77	12.25	11.42	0.83
C ₃ A	4.85	0.29	6.06	5.54	4.39	1.15
SiO ₂	20.85	0.32	1.56	21.55	20.33	1.22
Al ₂ O ₃	4.68	0.12	2.57	4.94	4.44	0.50
Fe ₂ O ₃	4.26	0.02	0.41	4.29	4.23	0.07
CaO	61.77	0.47	0.75	62.72	60.71	2.00
MgO	1.38	0.03	2.23	1.43	1.33	0.11
Na ₂ O	0.12	0.00	3.40	0.13	0.12	0.02
K ₂ O	0.20	0.02	10.61	0.24	0.16	0.08
SO ₃	2.93	0.13	4.43	3.23	2.66	0.56
Free lime	0.97	0.18	18.65	1.49	0.67	0.82
Alkaline equivalent	0.26	0.02	6.39	0.29	0.23	0.07

SD: Standard Deviation, CV: Variation Coefficient, Max: Maximum datum, Min: Minimum datum.

References

1. Maury-Ramírez, A.; Illera-Perozo, D.; Mesa, J.A. Circular Economy in the Construction Sector: A Case Study of Santiago de Cali (Colombia). *Sustainability* **2022**, *14*, 1923. [\[CrossRef\]](#)
2. Villagrán-Zaccardi, Y.; Pareja, R.; Rojas, L.; Irassar, E.; Torres-Acosta, A.; Tobón, J.; Vanderley, J. Overview of cement and concrete production in Latin America and the Caribbean with a focus on the goals of reaching carbon neutrality. *RILEM Tech. Lett.* **2022**, *7*, 30. [\[CrossRef\]](#)
3. Economía Circular—DANE. Available online: <http://www.andi.com.co/Uploads/economia-circular-1-reporte.pdf> (accessed on 6 April 2023).
4. Maury-Ramírez, A.; De Belie, N. Environmental and Economic Assessment of Eco-Concrete for Residential Buildings: A Case Study of Santiago de Cali (Colombia). *Sustainability* **2023**, *15*, 12032. [\[CrossRef\]](#)
5. Lemos-Micolta, E.D.; Chilito-Bolaños, L.C.; Maya-Soto, J.C.; Gómez-Gómez, A.; Rojas-Manzano, M.A. Uso de la Escoria de Aluminio en el Concreto—Revision del Estado del Arte. In Proceedings of the IX Congreso Internacional y 23a Reunión Técnica (AATH 2020), La Plata, Argentina, 2–6 November 2020.
6. Pereira, D.A.; de Aguiar, B.; Castro, F.; Almeida, M.F.; Labrincha, J.A. Mechanical behaviour of Portland cement mortars with incorporation of Al-containing salt slags. *Cem. Concr. Res.* **2000**, *30*, 1131–1138. [\[CrossRef\]](#)
7. Elinwa, A.U.; Mbadike, E. The use of aluminium waste for concrete production. *J. Asian Architect. Build Eng.* **2011**, *10*, 217–220. [\[CrossRef\]](#)
8. Reddy, M.S.; Neeraja, D. Mechanical and durability aspects of concrete incorporating secondary aluminium slag. *Resour. Effic. Technol.* **2016**, *2*, 225–232. [\[CrossRef\]](#)
9. Mailar, G.; Raghavendra, N.S.; Sreedhara, B.M.; Manu, D.S.; Hiremath, P.; Jayakesh, K. Investigation of concrete produced using recycled aluminium dross for hot weather concreting conditions. *Resour. Effic. Technol.* **2016**, *2*, 68–80. [\[CrossRef\]](#)
10. Panditharadhya, B.J.; Sampath, V.; Mulangi, R.H.; Shankar, A.U.R. Mechanical properties of pavement quality concrete with secondary aluminium dross as partial replacement for ordinary portland cement. *IOP Conf. Ser. Mater. Sci. Eng.* **2018**, *431*, 032011. [\[CrossRef\]](#)
11. Dai, C.; Apelian, D. Fabrication and characterization of aluminum dross-containing mortar composites: Upcycling of a waste product. *J. Sustain. Metall.* **2017**, *3*, 230–238. [\[CrossRef\]](#)
12. Parra-Molina, D. Estudio del Comportamiento Mecánico de Morteros con Sustitución Parcial de Cemento por Escoria de Aluminio y Efecto de la Reducción del Tamaño de Partícula. Master's Thesis, Universidad Javeriana Cali, Santiago de Cali, Colombia, 23 June 2023.
13. Sánchez De Guzmán, D. *Tecnología del Concreto y del Mortero*; Bhandar Editores: Bogotá, Colombia, 2001.

14. NTC-77; Método de Ensayo para el Análisis por Tamizado de los Agregados Finos y Gruesos. ICONTEC: Bogotá, Colombia, 2018.
15. NTC-237; Método de Ensayo para Determinar la Densidad Relativa (Gravedad Específica) y la Absorción del Agregado Fino. ICONTEC: Bogotá, Colombia, 2020.
16. NTC-176; Método de Ensayo para Determinar la Densidad Relativa (Gravedad Específica) y la Absorción del Agregado Grueso. ICONTEC: Bogotá, Colombia, 2019.
17. NTC-92; Método de Ensayo para la Determinación de la Densidad Volumétrica (Masa Unitaria) y Vacíos en Agregados. ICONTEC: Bogotá, Colombia, 1995.
18. NTC-33; Método de Ensayo para Determinar la Finura del Cemento Hidráulico por Medio del Aparato Blaine de Permeabilidad al Aire. ICONTEC: Bogotá, Colombia, 2019.
19. NTC-118; Método de Ensayo para Determinar el Tiempo de Fraguado del Cemento Hidráulico Mediante Aguja de Vicat. ICONTEC: Bogotá, Colombia, 2020.
20. NTC-110; Cantidad de Agua Requerida para la Consistencia Normal de una Pasta de Cemento Hidráulico. ICONTEC: Bogotá, Colombia, 2019.
21. NTC-221; Método de Ensayo para Determinar la Densidad del Cemento Hidráulico. ICONTEC: Bogotá, Colombia, 2019.
22. NTC-5784; Método de Ensayo para Determinar la Fluidez de Morteros de Cemento Hidráulico. ICONTEC: Bogotá, Colombia, 2021.
23. NTC-1926; Método de Ensayo para Determinar la Densidad (Masa Unitaria), el Rendimiento y el Contenido de Aire por Gravimetría del Concreto. ICONTEC: Bogotá, Colombia, 2013.
24. NTC-220; Determinación de la Resistencia de Morteros de Cemento Hidráulico a la Compresión, Usando Cubos de 50 mm o 2 Pulgadas de Lado. ICONTEC: Bogotá, Colombia, 2021.
25. NTC-120; Método de Ensayo para Determinar la Resistencia a la Flexión de Morteros de Cemento Hidráulico. ICONTEC: Bogotá, Colombia, 2022.
26. NTC-2017; Adoquines de Concreto para Pavimento. ICONTEC: Bogotá, Colombia, 2018.
27. Orozco-Eraza, D.A.; Vega-Báez, J.A. Estudio del Efecto del Tamaño de Partícula de Escoria de Aluminio Calcinada Utilizada como Reemplazo Parcial del Cemento en las Propiedades Mecánicas de Morteros. Bachelor's Thesis, Pontificia Universidad Javeriana Cali, Santiago de Cali, Colombia, September 2022.
28. Shinzato, M.C.; Hypolito, R. Solid waste from aluminum recycling process: Characterization and reuse of its economically valuable constituents. *Waste Manag.* **2005**, *25*, 37–46. [[CrossRef](#)] [[PubMed](#)]
29. Bravo-German, A.M.; Bravo-Gómez, I.D.; Mesa, J.A.; Maury-Ramírez, A. Mechanical Properties of Concrete Using Recycled Aggregates Obtained from Old Paving Stones. *Sustainability* **2021**, *13*, 3044. [[CrossRef](#)]
30. Ritchie, H.; Roser, M.; Rosado, P. CO₂ and Greenhouse Gas Emissions. Our World in Data. 2023. Available online: <https://ourworldindata.org/grapher/annual-co2-cement?tab=map> (accessed on 15 September 2023).
31. Global Consensus on Sustainability in the Built Environment—GLOBE. Decarbonising Global Construction. Available online: <https://www.rilem.net/globe> (accessed on 20 September 2023).
32. Muñoz-Velez, M.F.; Salazar-Serna, K.; Escobar-Torres, D.; Rojas-Manzano, M.A.; Gómez-Gómez, A.; Maury-Ramírez, A. Circular Economy: Adding value to the post-industrial waste through the transformation of aluminum dross for cement-matrix applications. *Sustainability* **2023**, *15*, 13952. [[CrossRef](#)]

Disclaimer/Publisher's Note: The statements, opinions and data contained in all publications are solely those of the individual author(s) and contributor(s) and not of MDPI and/or the editor(s). MDPI and/or the editor(s) disclaim responsibility for any injury to people or property resulting from any ideas, methods, instructions or products referred to in the content.